

We are IntechOpen, the world's leading publisher of Open Access books Built by scientists, for scientists

4,800

Open access books available

122,000

International authors and editors

135M

Downloads

Our authors are among the

154

Countries delivered to

TOP 1%

most cited scientists

12.2%

Contributors from top 500 universities



WEB OF SCIENCE™

Selection of our books indexed in the Book Citation Index
in Web of Science™ Core Collection (BKCI)

Interested in publishing with us?
Contact book.department@intechopen.com

Numbers displayed above are based on latest data collected.

For more information visit www.intechopen.com



Biomimetic Membranes as a Tool to Study Competitive Ion-Exchange Processes on Biologically Active Sites

Beata Paczosa-Bator¹, Jan Migdalski¹ and Andrzej Lewenstam^{1,2}

¹*Faculty of Material Science and Ceramics,*

AGH University of Science and Technology, PL-30059 Cracow

²*Centre for Process Analytical Chemistry and Sensor Technology 'ProSens',
Process Chemistry Centre, Åbo Akademi University, FIN-20500 Åbo-Turku,*

¹*Poland*

²*Finland*

1. Introduction

The change in membrane potential with time is of fundamental importance in cell biology. From the biological point of view we are interested in the mechanism of voltage dependent channel block and related ionic antagonism that happens on the ion-binding sites forming channel necks (Migdalski at al., 2003; Paczosa at al., 2004; Paczosa-Bator at al., 2006). We argue that by applying biomimetic approach, the processes invisible in routine membrane research could be “amplified” and exposed for further scientific exploration. In our case, this argument refers to electrical potential transients and/or local concentration redistributions provoked a competitive calcium/magnesium or potassium/sodium/lithium ions exchange on the biological sites. Voltage-activation of the N-methyl-d-aspartate (NMDA) receptor channel, allowing for calcium ion influx by relieving the block by magnesium ion (Nowak at al., 1984; McBain at al., 1994), or monovalent ion effects such as potassium-sodium/lithium/TEA(tetraethylammonium) in the case of potassium and sodium channels (Hille, 1992) is used to illustrate the value of biomimetic methodology.

From the electrochemical point of view, our strategy means an interest in the time-dependent (dynamic) characteristics of a membrane potential resulting from competitive ion-exchange processes. The membranes used in our studies are in electrochemistry known as the electroactive parts of ion-selective sensors sensitive for magnesium, calcium, potassium, sodium and lithium, which are the ions of our interest.

To bridge mentioned above biological and electrochemical interests we use biomimetic membranes. The novelty of our approach is in applying conductive polymers (CPs) as with purposely dispersed bioactive sites. This allows observation of a competitive (antagonistic) ion exchange and its coupling with a membrane potential formation process on biologically active sites (BL). The sites in focus of our research, adenosinetriphosphate (ATP), adenosinodiphosphate (ADP), heparin (Hep) and two amino acids – asparagine (Asn) and glutamine (Gln), competitively bind calcium, magnesium, lithium, sodium and potassium ions and thus play an important role in ion-dependent biological membrane processes (Saris

at al., 2000). In particular, ATP takes part in active membrane potential formation, Hep in the anticoagulation process (Desai, 2004) and Asn and Gln in the voltage-ligand gated influx on calcium ions via the NMDA channels (McBain & Mayer, 1994).

The following methodology is accepted for applying CPs as biomimetic membranes. In order to obtain the membranes (CP-BL-Y, where Y = K⁺, Na⁺, Li⁺, Ca²⁺, Mg²⁺), first ATP, ADP, Hep, Asn or Gln are introduced into the CP matrix during electropolymerization. Next, the calcium, magnesium, lithium, sodium or potassium potentiometric sensitivity is induced by soaking in an alkaline solution of one of these ions until close-to-Nernstian sensitivity for the films is obtained. The films are then used to monitor the equilibration processes induced by the change in bulk concentration of magnesium/calcium or lithium/potassium/sodium ions or stimulation with external electrical signal (Paczosa-Bator et al., 2009). The resulting transitory potential response is recorded and characteristic potential transients observed are theoretically interpreted.

2. Conducting polymers used and their properties

It is well known that conducting polymers (CPs) such as poly(pyrrole) (PPy), poly(N-methylpyrrole) (PMPy) or poly(3,4-ethylenedioxythiophene) (PEDOT) in the oxidation process during electrodeposition are easily doped with small inorganic anions and in consequence exhibit anionic open-circuit sensitivity.

Cationic sensitivity can be observed if the CP films are doped with cations during reduction. This happens when the CP film is doped with bulky immobile anions, for instance naphthalenesulphonate, indigo carmine or methylene blue (Gao et al., 1994; Bobacka et al., 1994). The ionic sensitivity induced in this way is dependent on the redox status of the polymer film and is rather nonselective (Lewenstam et al., 1994).

As we shown, the cationic sensitivity may be enhanced and stabilized with use of bulky, metal-complexing ligands from the group of metallochromic indicators as dopants. This happens because the bulky dopants retain in the polymer film their complexing properties known from water chemistry and the selective cationic sensitivity results from the complex formation inside CP films (Migdalski et al., 1996).

This provides the unique possibility of forming CP films doped with bulky and biologically active anions such as adenosinotriphosphate (ATP), adenosinodiphosphate (ADP), heparin (Hep) or amino acids – asparagine (Asn) and glutamine (Gln). These films may be used as biomimetic membranes to inspect processes important for membrane potential formation or membrane transport (Paczosa-Bator et al., 2007).

Our observations have shown that the conducting polymer designed for biomimetic membranes should have smooth surface morphology (a. Paczosa-Bator et al., 2006). It is well known that the morphology of conducting polymer films depends on many experimental parameters, such as substrate used, electrodeposition method, kind of monomer and doping anions, kind of solvent, pH and post deposition treatment of the film. Depending on the further application of conducting polymer layers, different surface morphology (rough or smooth) and different structure are required (Niu et al., 2001; Unsworth et al., 1992; Maddison & Unsworth 1989).

3. Materials and methods

The electrosynthesis of conducting polymer membranes on GC and ITO electrodes was carried out using an Autolab general Purpose System (AUT20.Fra2-Autolab, Eco Chemie,

B.V., Utrecht, The Netherlands) connected to a conventional, three-electrode cell. The working electrode was a glassy carbon (GC) disk with an area of 0.07 cm² or conducting glass pieces with an area of about 1 cm² (ITO, Lohja Electronics, Lohja, Finland, used for the FTIR, EDAX, XPS and LA-ICP-MS experiments). The reference electrode was an Ag/AgCl/3M KCl electrode connected to the cell via a bridge filled with supporting electrolyte solution, and a glassy carbon (GC) rod was used as the auxiliary electrode. The solutions used for polymerization contained selected monomer and an electrolyte that provided the doping ion. Electropolymerization was performed in solutions saturated with argon at room temperature.

The potentials were measured using a 16-channel mV-meter (Lawson Labs, Inc., Malvern, PA). The reference electrode was an Ag/AgCl/3M KCl electrode. All experiments were performed at room temperature.

The X-ray photoelectron spectroscopy (XPS) analysis was performed with a Physical Electronics Quantum 2000 XPS-spectrometer equipped with a monochromatized Al-X-ray source. The Energy Dispersive Analysis of X-ray (EDAX) measurements were performed using a Scanning Electron Microscope, SEM model LEO 1530 from LEO Electron Microscopy Ltd, which was connected to an Image and X-ray analysis system - model Vantage from ThermoNoran. The LA-ICP-MS measurements were performed using a model 6100 Elan DRC Plus of ICP-MS from Perkin Elmer SCIEX (Waltham, USA) and UP-213 of Laser Ablation from "New wave Research" Merchantek Products (Fremont, USA). The Fourier Transform Infrared (FTIR) spectra were recorded with a Bruker IFS 66/S instrument. The Atomic Force Microscopy (AFM) images were recorded with a NanoScope IIIa microscope (Digital Instruments Inc., Santa Barbara, CA), equipped with the extender electronics module enabling phase imaging in tapping mode. For numerical calculations Mathcad 2001 Professional by MathSoft, Inc. Canada, was used.

4. Procedures of CP-BL-Me electrode preparation

4.1 Conducting polymer films - deposition

The electrodeposition of the poly(pyrrole), poly(N-methylpyrrole) or poly(3,4-ethylenedioxythiophene) films was carried out from solution that contained dopant and selected monomer. The monomer concentration was equal to 0.1M for pyrrole and N-methylpyrrole or 0.01 M for 3,4-ethylenedioxythiophene. Dopant concentration was equal to 0.1M for ATP, ADP, Gln or Asn. PEDOT, PMPy and PPy were electrodeposited onto the working electrode potentiostatically, under constant potential or dynamically with potential cycling. In the last case the scan rate was equal to 20 mV·s⁻¹. Deposition time or number of cycles was selected to obtain desired charge density.

CP films doped with ATP and ADP were deposited potentiostatically under +0.9 V or +1.02 V (PEDOT), +0.66, 0.68 or +0.70 V (PPy) as well as +0.8 V (PMPy) (vs. Ag/AgCl/3M KCl) or dynamically by scanning the potential in the range 0 - (+0.9) V or 0 - (+1.02) V (PEDOT films) and 0 - (+0.70) V (PPy films) (vs. Ag/AgCl/3M KCl). The charge density was equal to 510 - 750 mC·cm⁻².

PPy-Asn(Gln) films were grown on the working electrode at a potential of +1.00 V (vs. Ag/AgCl/3M KCl) and charge density of 240 mC·cm⁻² was used.

The growth of heparin-doped poly(pyrrole) and poly(3,4-ethylenedioxythiophene) was performed using solutions containing 40 mg·ml⁻¹ of heparin and 0.1 M pyrrole or 0.01M 3,4-ethylenedioxythiophene. Dynamic growth was performed by scanning the potential

between 0 and +0.80 V (PPy) or 0 and +0.92 V (PEDOT) (vs. Ag/AgCl/3M KCl) and potentiostatic growth was achieved by holding a potential at +0.80 V (PPy) and +0.92 V or +0.96 V (PEDOT) (vs. Ag/AgCl/3M KCl) for different times in order to obtain charge density 480 – 840 mC·cm⁻².

4.2 The process of making CP-BL membranes cation-sensitive

After synthesis, the polymer membranes were washed with deionized water and then the electrodes were soaked and stored in a alkaline mixture of 0.1 M YCl_n and $Y(OH)_n$ where Y was a main cation. Only conditioning in the alkaline solution was effective. The cation complexes with BL were formed after CP-BL film deprotonation in alkaline solutions (protons were substituted with other cations) as shown on Fig. 1. As a rule, a cationic response with a linear range within the K^+ , Na^+ , Li^+ activities from 10^{-1} M to 10^{-4} M and Ca^{2+} , Mg^{2+} activities from 10^{-1} M to 10^{-5} M with a close-to-Nernstian slope was observed for the CP-BL films usually after 1 week of soaking.

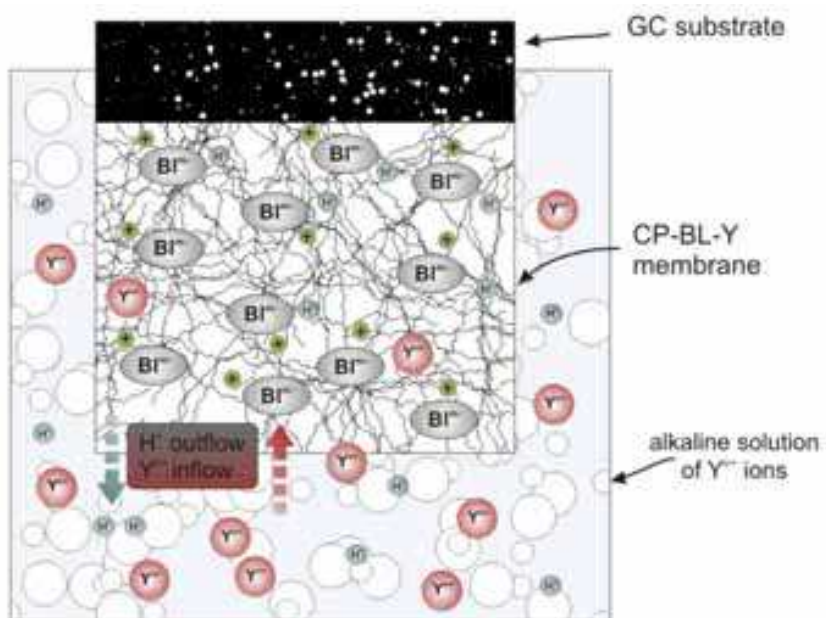


Fig. 1. Ion-exchange processes during conditioning of CP-BL membrane in alkaline solution.

5. Results and discussion

5.1 Electrodeposition and its influence on potentiometric response

The short response time of the CP-BL membranes is highly desirable to study the transient membrane potential changes during equilibration processes. As we have shown for CP-ATP membranes, the response time is strongly dependent on the film morphology. The AFM and potentiometric study conducted in parallel have exemplified the strong influence of the film preparation conditions on its further potentiometric response.

Generally, CP-BL films made under dynamic conditions are close to two dimensional structures i.e. they are flat and compact, while the potentiostatic deposition leads to three-dimensionally morphology of the films. Fig. 2 presents the exemplary AFM phase contrast images of the PPy-ATP membranes taken after film deposition under different conditions: potentiostatic under +0.66 V (a), +0.68 V (b), +0.70 V (c) and dynamic (0- (+0.7) V) (d). The

size of each image is equal to $3\ \mu\text{m} \times 3\ \mu\text{m}$ and the thickness of all compared films was equal to $2\ \mu\text{m}$.

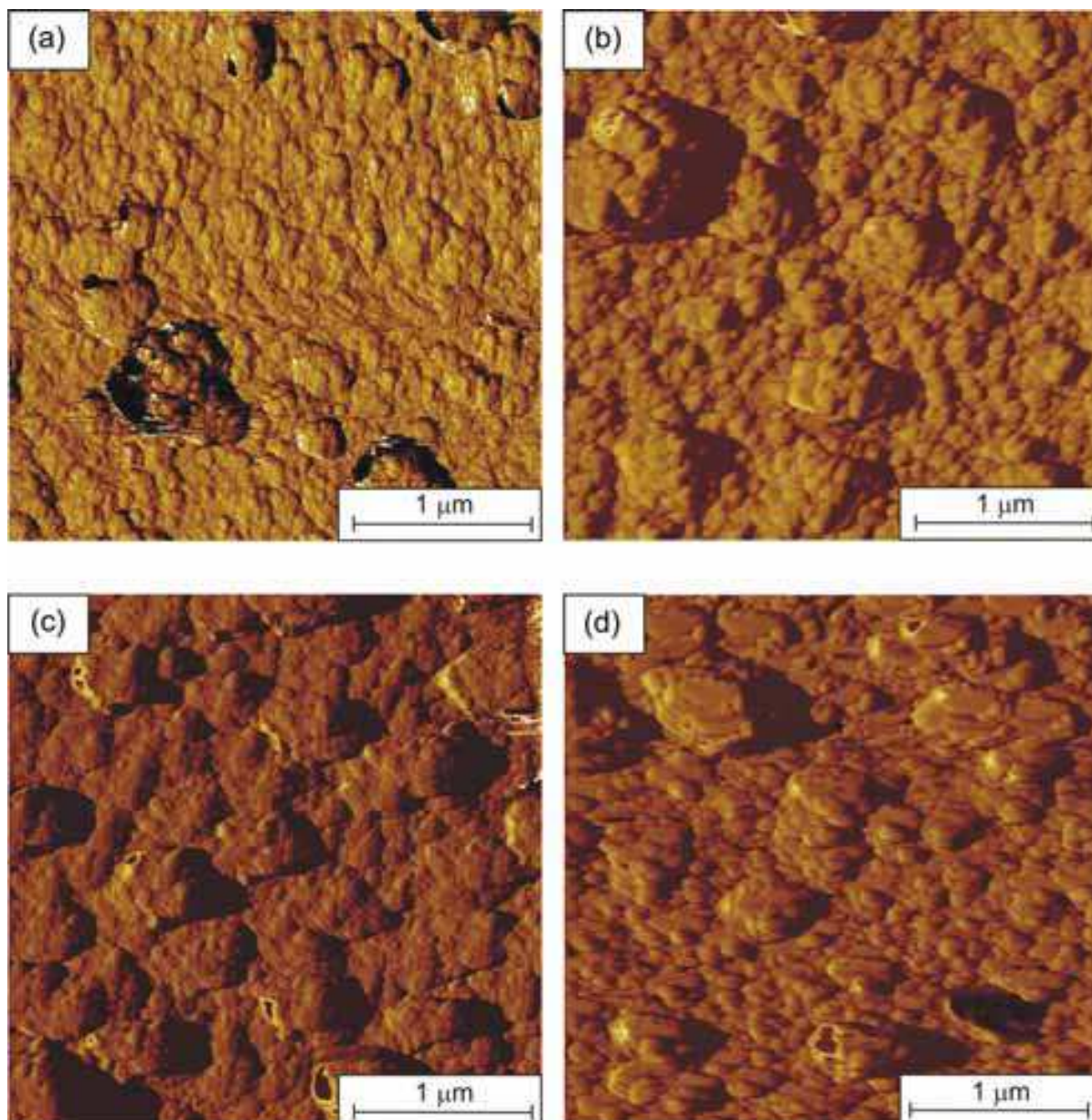


Fig. 2. AFM phase contrast images of the PPy-ATP layers prepared by electropolymerization under different conditions: potentiostatic under (a) +0.66 V, (b) +0.68 V, (c) +0.70 V and (d) dynamic with potential cycling between 0 and +0.70 V. The size of each image is $3\ \mu\text{m} \times 3\ \mu\text{m}$.

As shown in Fig. 2(b) and 2(c), the PPy layers prepared potentiostatically under +0.68 V and +0.70 V exhibit quite rough surface (large RMS roughness (S_q) and ten-point height (S_z)) with relatively high effective surface area (S_{dr}), see Table 1. In contrast, the membrane prepared by potential cycling were smoother (smaller S_q and S_z) as well as have smaller effective surface area Fig. 2(d). The membranes prepared by potentiostatic method but under the lowest potential +0.66 V (Fig. 2(a)) show the smoothest surface and the densest structure (the smallest value of RMS and the highest value of skewness (S_{sk})). The films

prepared under higher potentials have a less compact structure with more porous surface (smaller value of skewness (S_{sk})), resulting from rapid film growth, and have a less glossy appearance.

Method and potential of electrodeposition	Potentiostatic +0.66	Potentiostatic +0.68	Potentiostatic +0,70	Dynamic 0 - (+0,70)
Scan size, $\mu\text{m} \times \mu\text{m}$	3×3	3×3	3×3	3×3
S_q , nm	70.4	78.1	81.1	72.7
S_z , nm	426	481	500	423
S_{sk} , -	3.16	2.03	1.64	1.32
S_{dr} , %	28.7	36.6	38.1	30.2

Table 1. Roughness analysis of AFM images shown in Fig. 2: S_q (RMS roughness) and S_z (average of 5 minima and 5 maxima); S_{sk} (skewness); S_{dr} (effective surface area).

A comparison of the responses time of CP-BL membranes prepared by different methods (namely, potentiostatically and dynamically) proves that the surface of the polymer films greatly influence this parameter. After 2 weeks of conditioning, the films prepared by potential cycling and under potentiostatic conditions with the smallest potential, (which showed the most smooth surface among all films studied), were characterized by the shortest response time ($t_{90} \approx 7-10$ s), in contrast to the films obtained potentiostatically with +0.68 and +0.70 V ($t_{90} \approx 70-95$ s). After 4 months of soaking the response time of all studied electrodes have become similar ($t_{90} \approx 5-8$ s). PPy-ATP membranes with more compact structure required longer conditioning to induce the theoretical cationic response (in comparison with porous PEDOT-ATP membranes that show value of skewness close to 0 or negative as we showed in b. Paczosa-Bator at al., 2006). PPy-BL membranes exhibit also longer response time in comparison with PEDOT-BL. Exemplary potentiometric response of calcium sensitive PEDOT-ATP membranes taken after 2 weeks of conditioning in alkaline calcium solution is shown on Fig. 3. It is evident that different parameters of electropolymerization, and subsequent soaking, influence the potentiometric response of CP-BL films.

The thickness of CP-BL membranes also influence their potentiometric sensitivity. For example, calibration curves recorded for PEDOT-ATP membranes with different thickness taken after 1 month of soaking with alkaline calcium solution are shown on Fig. 4. As can be seen, from Fig. 4, thinner membranes showed narrow linear range (only from 10^{-5} to 10^{-3} M) and thicker membranes need longer time of conditioning in order to induce cationic response (even 2 months). The obtained results have shown that optimal thickness of membranes deposited under potentiostatic conditions was 2 μm but for the membranes prepared by potential cycling the optimal thickness was between 2 - 4 μm .

Generally the best cationic response with linear and the close-to-Nernstian slope value in the range 10^{-1} M - 10^{-4} M (for monovalent cations) or 10^{-1} M - 10^{-5} M (for divalent cations) was observed for membranes obtained dynamically with thickness 2-4 μm .

Freshly deposited and unsoaked CP-BL electrodes did not respond to studied ions (potassium, sodium, lithium, calcium and magnesium). In order to induce potentiometric sensitivity, the CP-BL membranes were conditioned in the alkaline solution containing chosen cations.

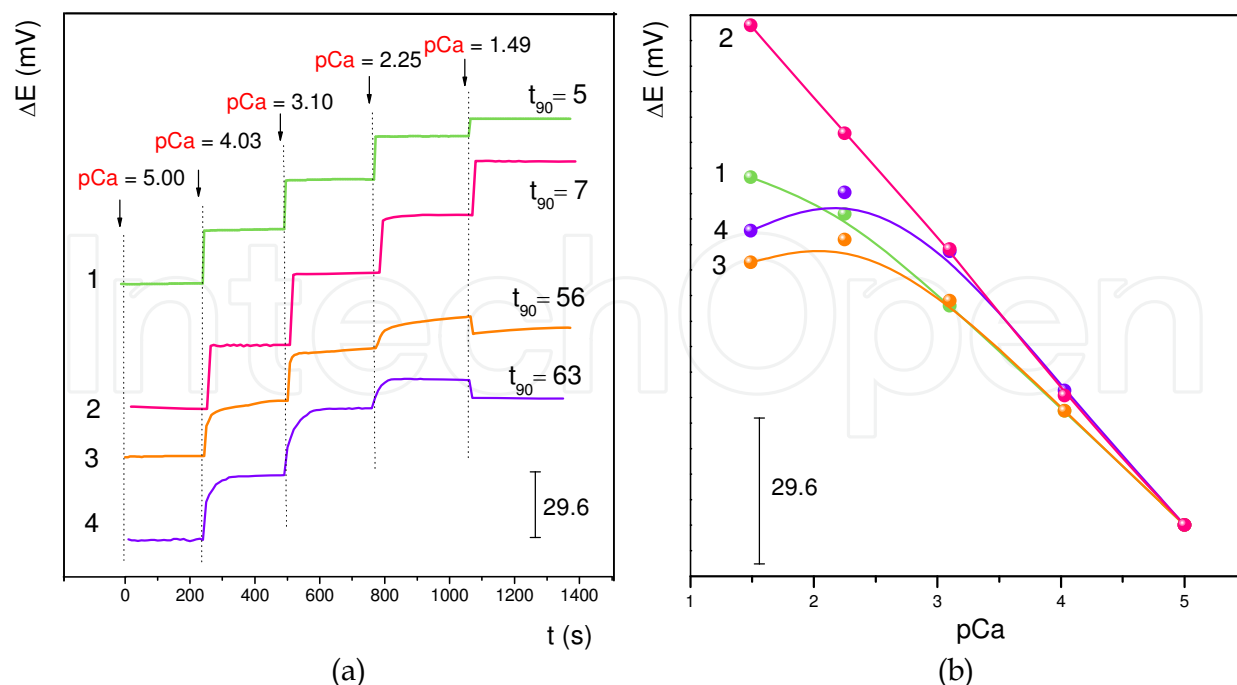


Fig. 3. Comparison of the potentiometric responses of the PEDOT-ATP electrodes performed after two weeks of soaking with alkaline calcium solution for membranes deposited under different conditions: dynamically by cyclic the potential between (1) 0 and +0.90 V, (2) 0 and +1.02 V and potentiostatically under (3) +0.90, (4) +1.02 V.

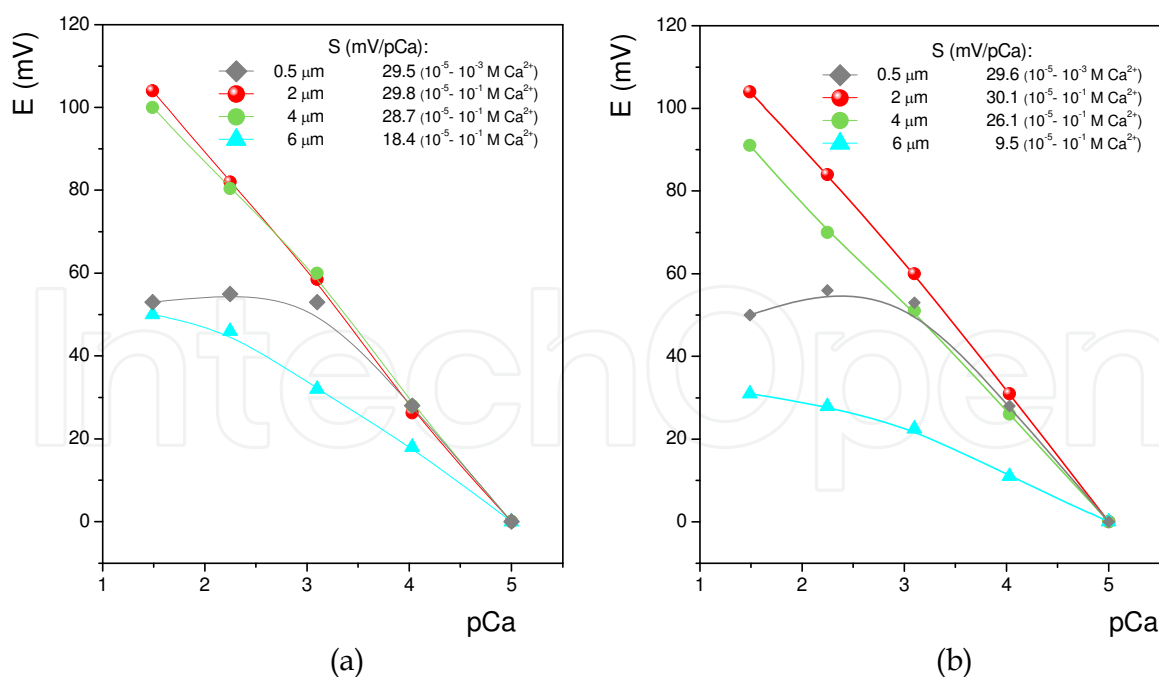


Fig. 4. Comparison of the potentiometric responses of the PEDOT-ATP films with different thickness and deposited under different conditions. Deposition conditions: (a) dynamically by cyclic the potential between 0 and +0.90 V, (b) potentiostatically under +0.90 V. Calibrations with CaCl₂ were performed after 1 month of soaking with alkaline calcium solution.

The response of CP-BL membranes was tested in chloride salts of different cations. Usually, after 1-2 weeks of soaking in alkaline solution of sodium, potassium, lithium, calcium or magnesium ions CP-BL membranes exhibit close to theoretical slope value. Fig. 5 presents the influence of soaking period on cationic sensitivity of the PPy-ATP membranes conditioning in different main ions solutions. Similar behaviour was observed for the all CP-BL membranes.

Induced cationic sensitivity was very stable even after using considerably long period of soaking (6-8 months). For example, the slope values for PPy-heparin and PEDOT-ATP films prepared potentiostatically at low potential, adequately +0.66 V and +0.90 V were equal to 29.24 ± 1.01 mV/pMg and 28.56 ± 1.12 mV/pCa during 8 months of PPy-heparin membranes conditioning and 58.92 ± 0.62 mV/pK, 57.58 ± 0.92 mV/pLi and 59.12 ± 0.42 mV/pNa during 6 months of PEDOT-ATP films soaking. It should be noted that all measurements were performed for the same thickness of films ($2 \mu\text{m}$).

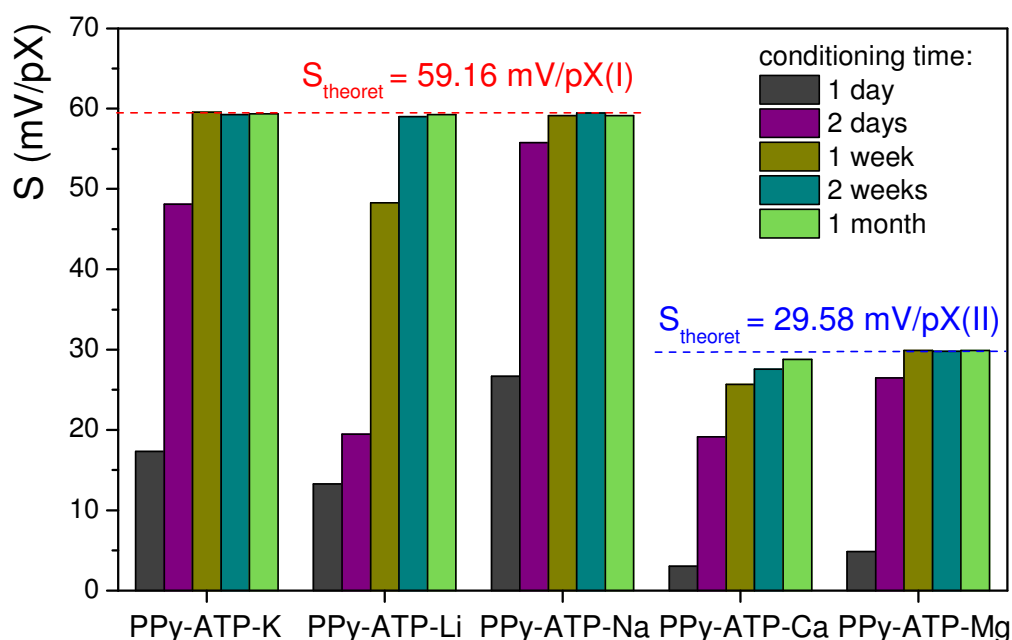


Fig. 5. Influence of soaking period on cationic sensitivity of PPy-ATP membranes (S is the obtained slope value).

5.2 Influence of soaking (conditioning) on the surface morphology of biomimetic membranes

In order to study possible topographic changes during soaking of the CP-BL membranes, AFM topography images were registered for freshly deposited films as well as after different period of soaking in alkaline solution.

Fig. 6 shows exemplary AFM images recorded for PPy-heparin membranes prior to and after soaking in alkaline magnesium solution for one week and one month. These images provide evidence that the conditioning process greatly influences the surface topography. The roughness parameters S_q and S_z clearly show that the films become smoother after conditioning (Table 2). Simultaneously, the effective surface area of the films decreases, most considerably between 1 week and 1 month of soaking (see Fig. 6 and Table 2). The phase contrast images nicely reveal the structural boundaries not so clearly visible in the

topographs. They demonstrate that the peaks or spheroidal growths observed before conditioning disappear as a result of conditioning. The skewness (S_{sk}) values confirm this change, changing from positive (Fig. 6a) to negative (Figs. 6b,c) values during conditioning. The surface hence changes from that dominated by peaks (Fig. 6a) to a Gaussian (Fig. 6b) or even porous (Fig. 6c) surface (Table 2).

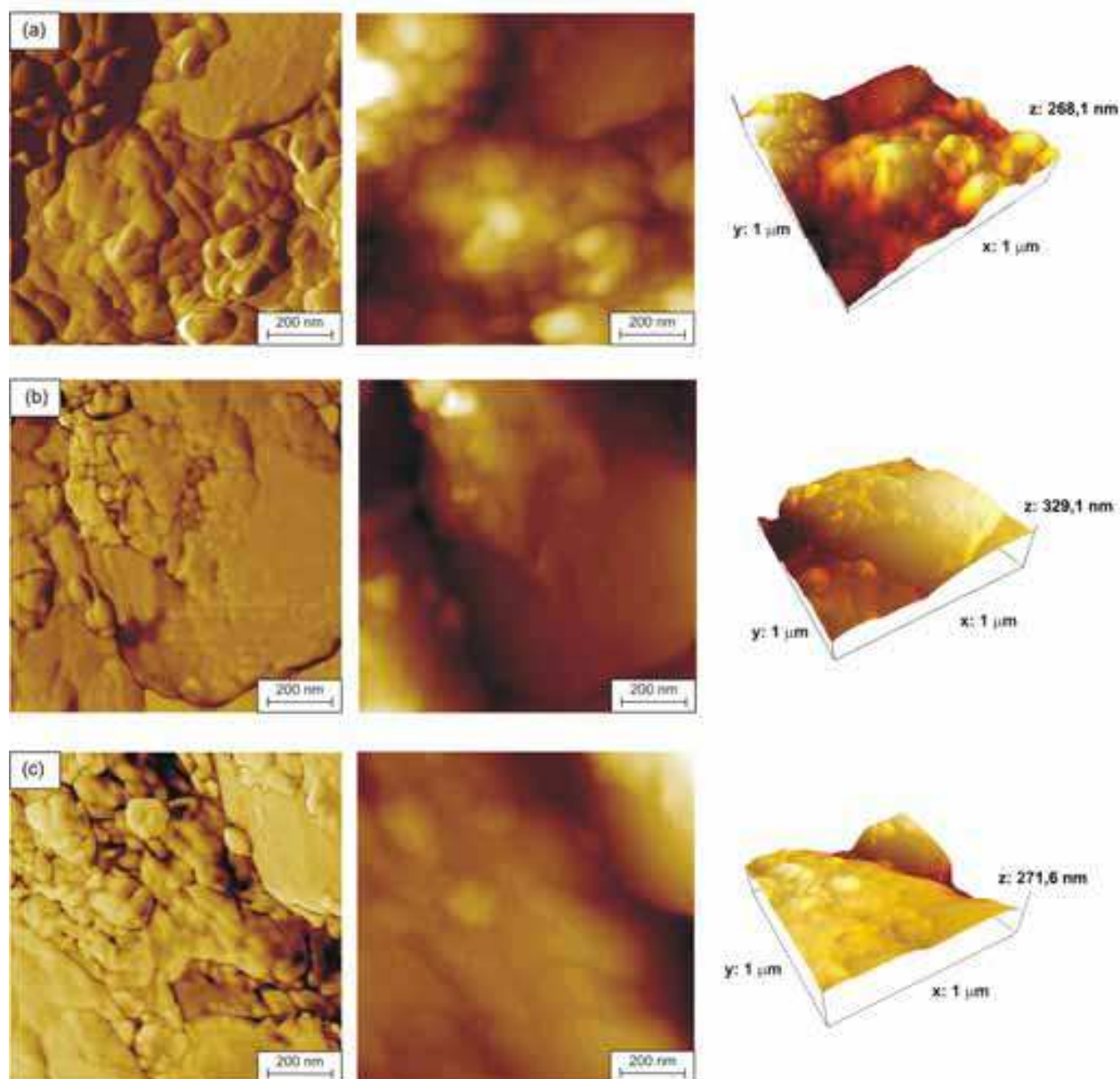


Fig. 6. AFM phase contrast topography and three-dimensional images of PPy membranes prepared potentiostatically at +0.80 V: (a) before conditioning and after conditioning in alkaline magnesium solution for 1 week (b) and 1 month (c).

The size of each image is $1 \mu\text{m} \times 1 \mu\text{m}$.

A long time soaking does not result in any “mechanical disintegration” of the films due to overoxidation, but makes the polymer surface smoother. At the same time the response time became shorter (see paragraph 4.1.). In consequence, a long time of soaking results in CP-BL films showing very similar potentiometric responses, irrespective on deposition method used.

Time of post-deposition conditioning	-	1 week	1 month
Scan size, $\mu\text{m} \times \mu\text{m}$	1×1	1×1	1×1
S_{qr} , nm	68.1	59.4	42.7
S_{zr} , nm	165	135	120
S_{skr} , -	1.66	-0.75	-1.35
S_{dtr} , %	25.1	19.11	8.1

Table 2. Roughness analysis of AFM images shown in Fig. 6.

5.3 Chemical characterization of polymer films

The elemental analysis of CP-BL membranes was performed using four different methods: Fourier transform infrared spectroscopy for membranes doped with amino acids, X-ray photoelectron spectroscopy and energy dispersive analysis of X-ray for CP-BL films sensitive towards divalent ions and laser ablation inductively coupled plasma mass spectrometry for CP-BL films sensitive towards monovalent ions to assess qualitatively the deposition process and influence of soaking on the composition of these membranes.

For the chemical and morphological analysis two kinds of samples were prepared namely: CP-BL without soaking and CP-BL after 2 weeks of soaking in the solution of main ions.

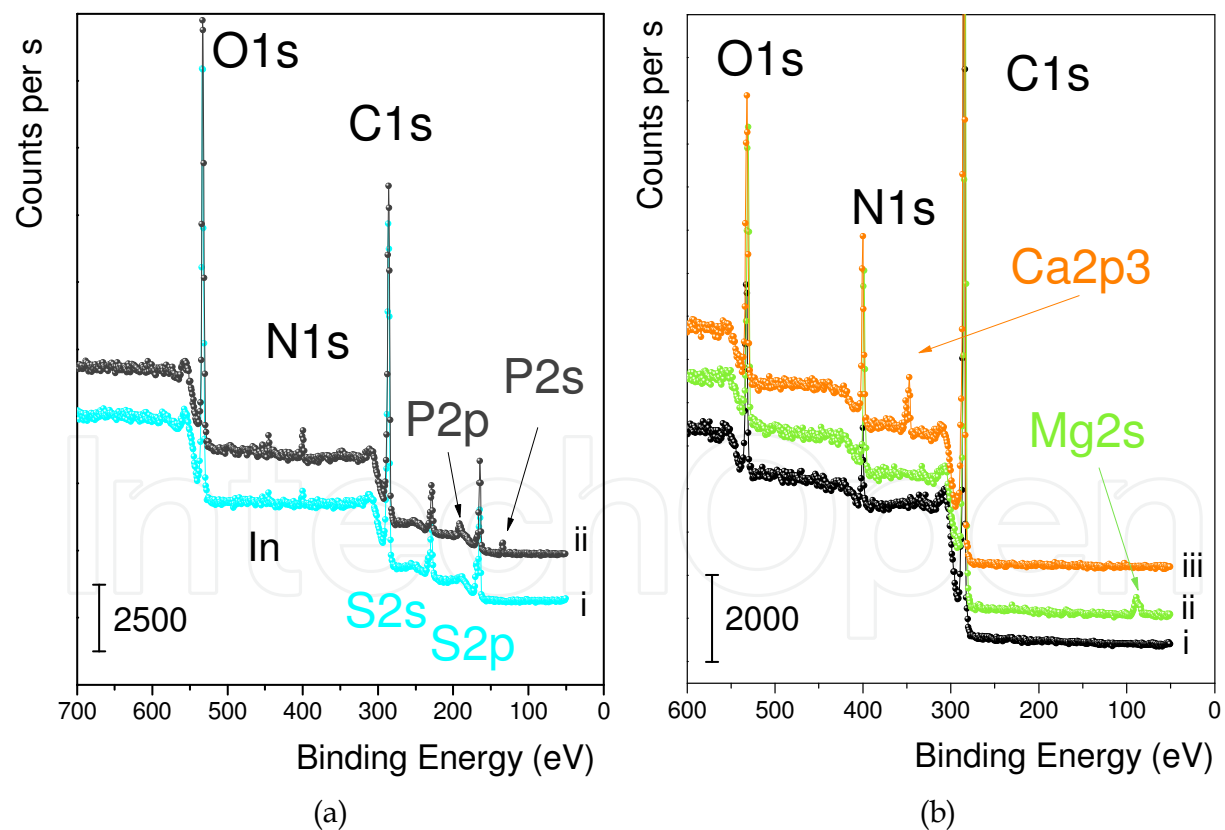


Fig. 7. The exemplary XPS spectra recorded for (a) PEDOT-heparin (i curve) and PEDOT-ATP (ii curve) membranes and (b) PPy-Asn membranes: i) freshly deposited and unsoaked, ii) after conditioning in alkaline magnesium solution, iii) after conditioning in alkaline calcium solution.

The presence of the phosphorus signal in the case of CP-ATP films in the XPS and LA-ICP-MS spectra as shown in Fig. 7a (ii curve) and Fig. 8b proves that counter-ions dope the films formed during electrodeposition (in the case of PEDOT membranes, ATP presence additionally proves nitrogen peak originating from this counter-ion. The heparin in the polymer matrix was identified by presence of nitrogen peak (in the case of PEDOT membranes) or sulfur peak (in the case of PPy membranes) as shown on Fig. 7a (i curve) and Fig. 8a. On the FTIR spectra of the PPy-amino acid films, a large absorbance band in the NIR region caused by the oxidized state of PPy was observed. The spectra of the poly(pyrrole) films showed a C=O stretching - vibration peak at 1651 cm^{-1} , O-H at 1260 cm^{-1} , O-C=O near 800 cm^{-1} and 725 cm^{-1} assigned for Gln or Asn.

The EDAX and XPS analysis of CP-BL films showed that after the conditioning process also calcium or magnesium peaks had appeared on the spectrum (as show exemplary for PPy-Asn membranes on Fig. 7b and PEDOT-Heparin membranes on Fig. 8a).

The LA-ICP-MS measurements for the CP-BL sample sensitive toward monovalent ions proved that after the conditioning desired cations were present in the membranes, e.g. after conditioning in alkaline lithium solution the potentiometric sensitivity towards these ions had been induced and the LA-ICP-MS spectrum showed a lithium signal (which was not observed before the conditioning process) as presented in Fig. 8b. The same behaviour was observed for potassium and sodium ions.

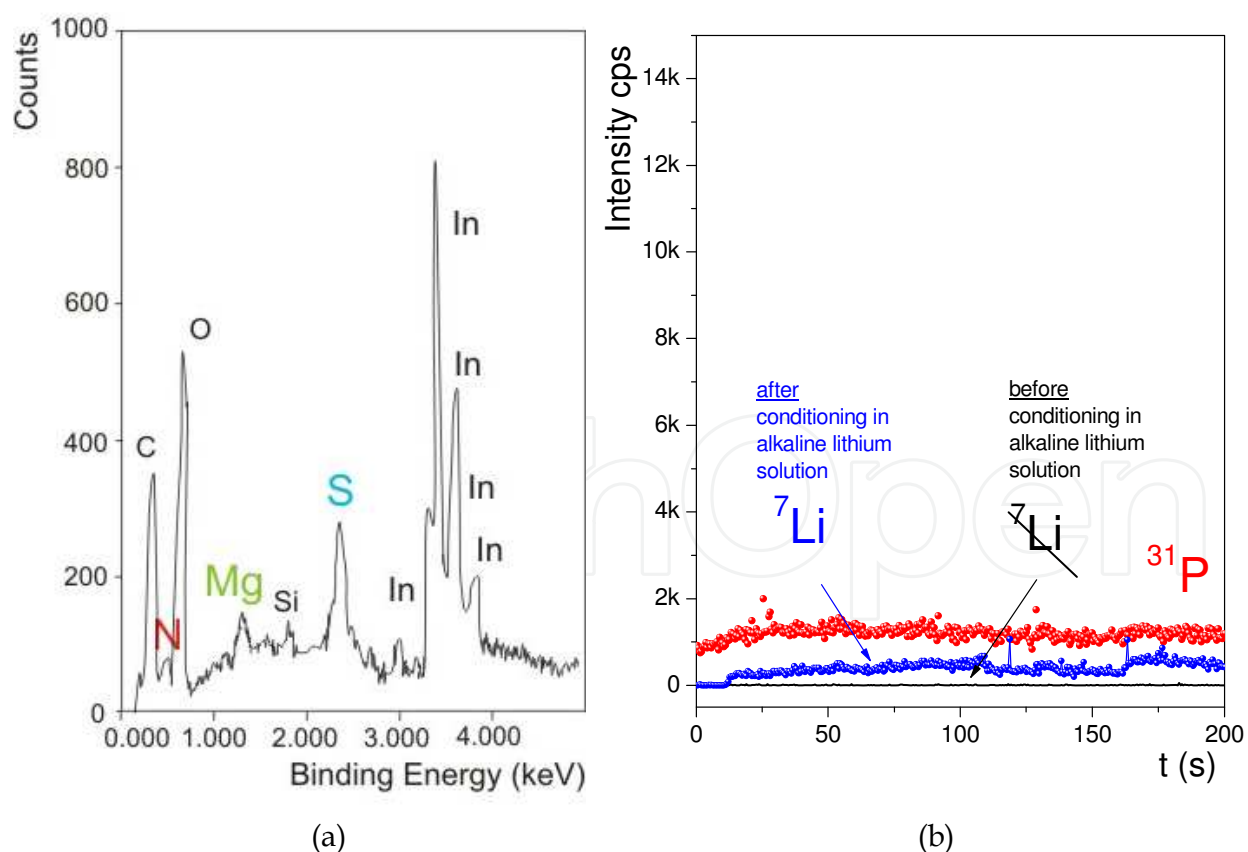


Fig. 8. The exemplary EDAX spectrum of PPy-Heparin-Mg membrane (a) and LA-ICP-MS spectra recorded for PMPy-ATP films before and after conditioning in alkaline lithium solution (b).

5.4 Influence of interfering cations on biomimetic CP-BL membranes

After inducing a proper sensitivity the influence of other ions on biomimetic membranes potential was studied by adding the interfering ions to the solution of main ions. As expected, in the case of membranes sensitive towards monovalent cations, strong interferences of divalent cations were observed. Divalent cations-sensitive membranes were insensitive towards sodium, potassium or lithium ions, but strong interferences from cations forming a stronger complex with BL (e.g. Zn(II) or Cu(II)) were observed (as exemplary shown on Fig. 9). Importantly, the selectivity coefficient values for the membranes sensitive to divalent cations $K_{Mg,Ca}$ and $K_{Ca,Mg}$ as well as sensitive to monovalent cations $K_{Na,Li}$, $K_{Na,K}$, $K_{Li,K}$ were close to 1. This manifestation of similar thermodynamic properties of ions (in the groups studied), and makes any dissimilarity on the response attributed to the kinetic properties of these ions in the membrane systems studied.

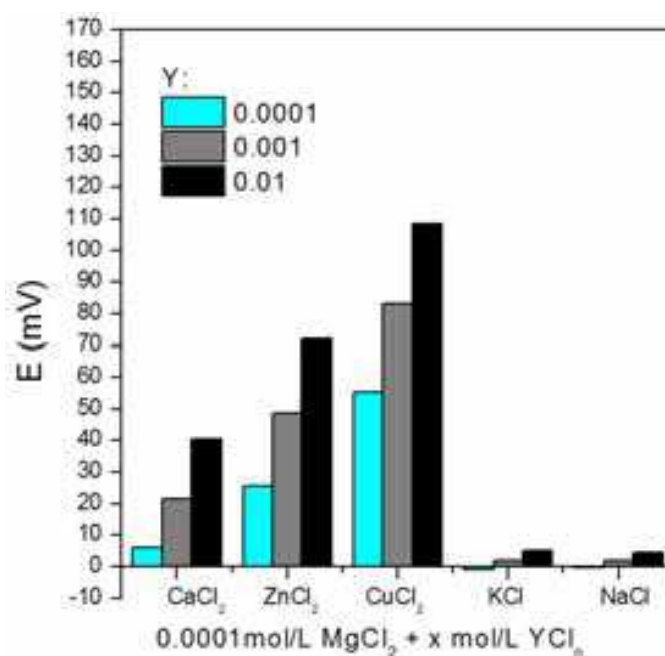


Fig. 9. The exemplary potential-response of PPy-Heparin membrane sensitive towards magnesium ions at interfering ions presence.

6. Ion competition and transient open-circuit response

In spite of similar sensitivity and selectivity of both groups of polymer films (namely, CP-BL-Ca(Mg) or CP-BL-K(Li)(Na)) towards divalent ions (calcium and magnesium) ions or monovalent ions (sodium, potassium and lithium), the transitory potential provoked by the changes in bulk concentrations of these groups of ions was strikingly different.

The representative plots for the measurements made for monovalent and divalent ion-sensitive membranes are shown on Fig. 10, for example PMPy-ATP-Na, PMPy-ATP-K and PPy-Asn-Ca(Mg) electrodes.

As can be seen from Fig. 10, potential-time ($E-t$) response strongly depends on the kind of ion that was involved in the competitive ion-exchange equilibration process. Lithium ion-exchange with sodium-rich CP-ATP-Na membranes results in a monotonic response (Fig. 10a), while if potassium ions are engaged in the ion exchange, instead of lithium, a non-monotonic (overshoot-type) response is observed (Fig. 10b). If sodium-rich membrane is

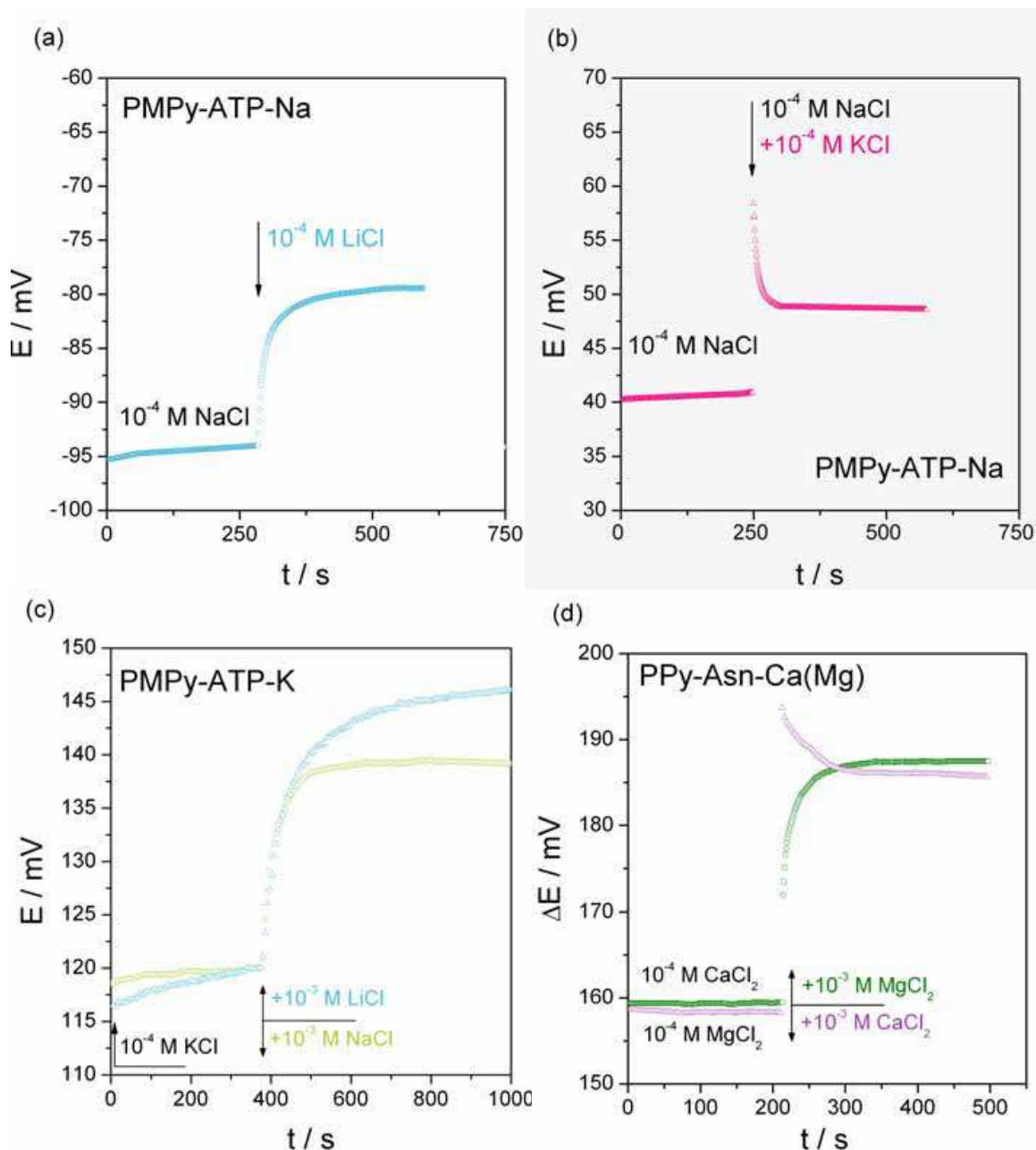
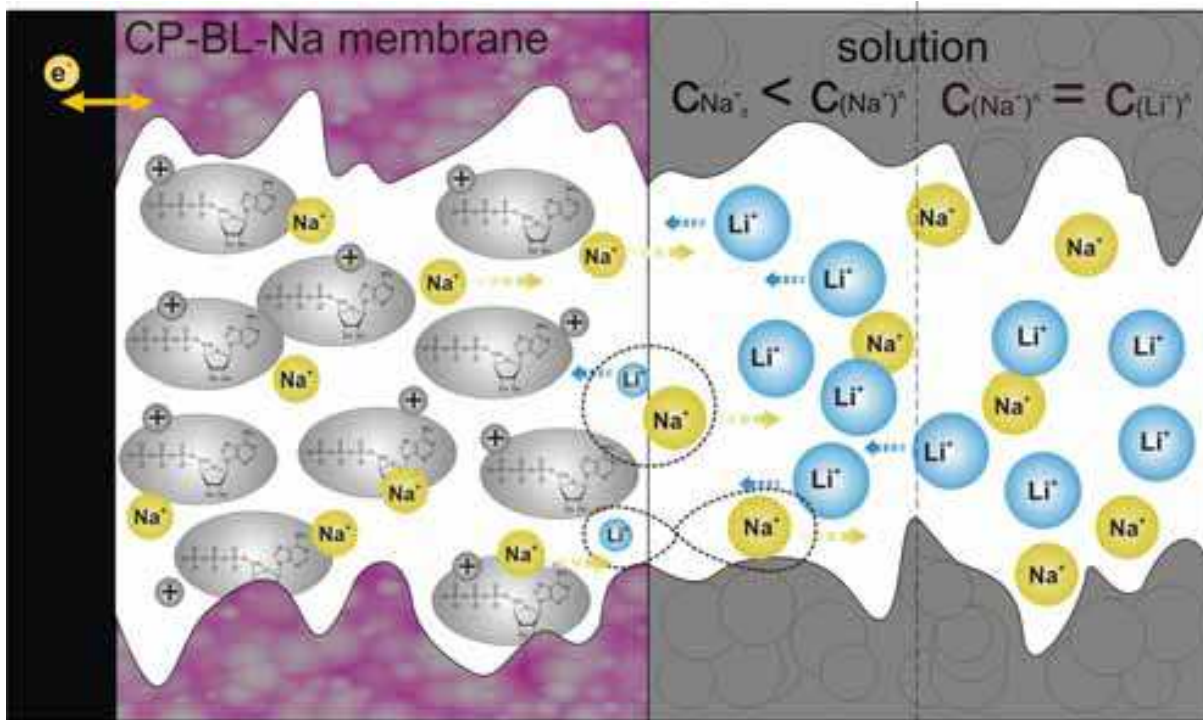
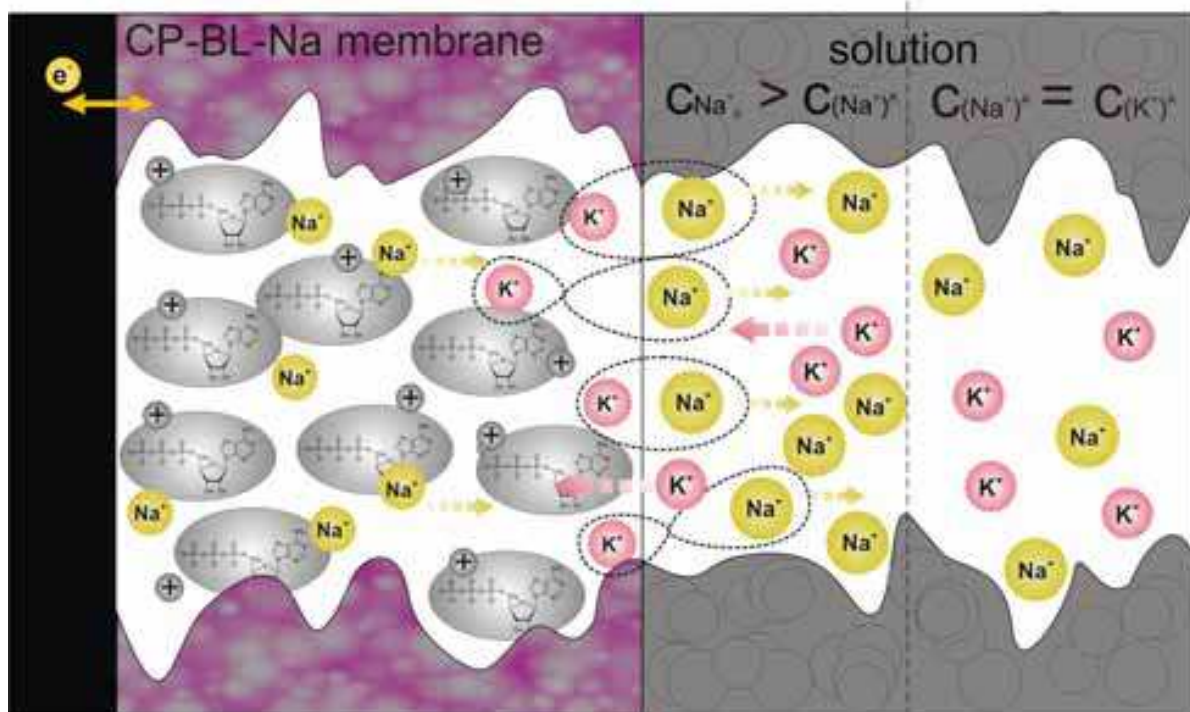


Fig. 10. Potential-time behaviour of sodium (a-b), potassium (c) sensitive PMPy-ATP and calcium and magnesium (d) PPy-Asn films observed after increase of a bulk concentration of: (a) Li^+ , (b) K^+ , (c) Li^+ (triangles), Na^+ (circles), (d) Ca^{2+} (triangles), Mg^{2+} (circles) ions.

converted to a potassium-rich one, then both a lithium and sodium response, as expected, is monotonic (Fig. 10c). A similar pattern is observed for CP-ATP-Mg membrane (Fig. 10d). Changes in bulk concentrations of magnesium ion are always associated with monotonic potential changes, while changes in concentration of calcium ions are associated with overshoot-type responses. These characteristic differences between potassium, sodium and lithium, as well as magnesium and calcium can be called “ionic antagonism”. Interestingly, and most probably not coincidentally, the same pairs of ions, i.e. Ca^{2+} - Mg^{2+} , Na^+ / Li^+ - K^+ , are indeed considered as antagonistic in real biological membrane systems, and specialized voltage and/or ligand-gated ion channels engaging these ions, e.g. NMDA.



(a)



(b)

Fig. 11. The simplified view of ion-exchange processes on CP-ATP-Na electrode in the mixed solution of primary (Na^+) and interfering ions after (a) lithium and (b) potassium concentration change.

As stated above, when discussing the selectivity of the membranes used, conventional interpretation based on thermodynamic equilibrium does not allow predicting any striking

difference in membrane responses. This fact lends credence to kinetic aspects in signal formation. A different rate in the transport of ions to and from the bioactive sites contributes to the effects observed. In other words, ion-exchange at the interface between bathing solution and membrane containing the sites and the ion transport are the source of the “antagonism” observed (Paczosa-Bator et al., 2007). The hypothesis is that faster ions (Ca and K characterized by the mobility 6.17 and $7.62 \cdot 10^{-8} \text{ m}^2\text{s}^{-1}\text{V}^{-1}$ respectively (Fraústo da & Williams, 2001) coming from the solution bulk and substituting via ion exchange slower ions from the film sites (Mg, Na and Li characterized by the mobility 5.49 , 5.19 and $4.01 \cdot 10^{-8} \text{ m}^2\text{s}^{-1}\text{V}^{-1}$ respectively (Fraústo da & Williams, 2001)) which allow for local accumulation of slower ions in the vicinity of membrane interface. And vice-versa if slower ions come from the solution to the film containing faster ions a deficit of this ion can be observed near to membrane surface. This mechanism is schematically illustrated for $\text{Na}^+\text{-K}^+$ and $\text{Na}^+\text{-Li}^+$ ions pair in Fig. 11.

7. Ion competition during stimulation with external electrical signal

As shown in Fig. 10, the changes in bulk concentration of ions result in characteristic changes of potential vs. time, and are attributed, as shown in Fig. 11, to local redistributions of ions in the vicinity of the membrane-solution interface. It is of great interest to convert the problem and ask whether one could observe any manifestation of this process in the experiment where the membrane ion redistribution is provoked by external electric signal, potential impulse. In this respect, in the absence of a method for direct visualization of the ionic concentration changes in the vicinity of membrane interface, a chrono-amperometric method was used. In this method, the external potential ($+5/-5$ and $+10/-10$ mV from the open-circuit potential) was applied to provoke ion fluxes to and from the membrane, and the fluxes are characterized by (ionic) current changes over time. It would be expected that after stimulation with external electrical signal faster ions (potassium or calcium) would produce currents that come to a base-line faster than in the case with ions of lower mobility (sodium/lithium or magnesium). The current response of the PMPy-ATP-Na electrode with time was measured in solutions of chloride salt of sodium, lithium and potassium with concentration equal to 10^{-4} M under different values of potential. In Fig. 12, the current-time (I-t) responses for sodium sensitive PMPy-ATP membrane are shown. The plots indeed prove the interrelation between the size of ions (resp. mobility of ions) and the I-t signal measured.

For the faster potassium ion (resp. calcium ion), after bigger initial cathodic or anodic current values a fast current drop was observed, while for slower sodium and lithium (resp. magnesium) ions the initial current were smaller and followed by slower current drop. This amperometric behaviour can be attributed to different mobility “antagonistic” ions. It can be concluded that transient response of the biomimetic membrane observed both in the open circuit and as well as under potential stimulation is dictated by different mobility of the ions. The kinetic difference is thus a prerequisite of the “ionic antagonism”.

8. Theoretical interpretation and implications

The change in membrane potential over time provoked by bulk concentration changes is attributed to local redistributions of ions at the membrane-solution interface and ion transport to and from this interface. If the membrane potential is changed by an external

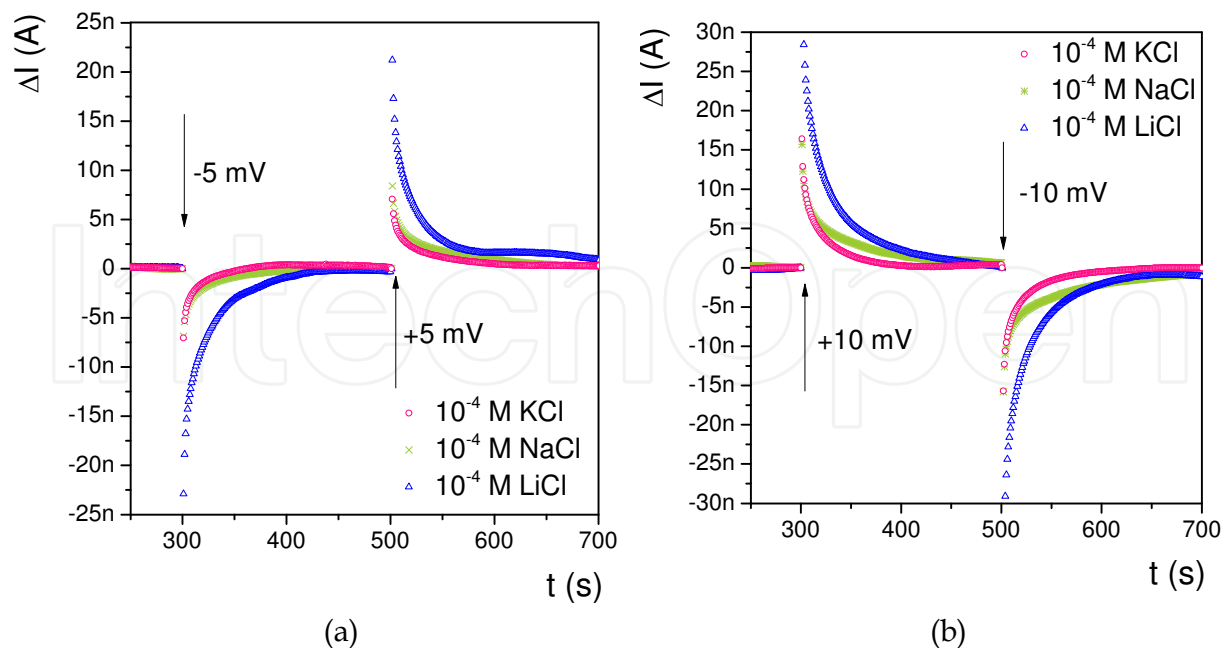


Fig. 12. The current (I) - time (t) response of PMPy-ATP-Na electrode recorded in chloride salt of the main and interfering ions under different value of potential (a) first -5 mV then +5 mV (b) + first +10 mV then -10 mV.

source resulting ionic fluxes could be observed and the ionic currents depend on the physicochemical properties of the ions engaged. These observations allow development of a general interpretation of E-t response for this biomimetic system using the Nernst-Planck-Poisson model (NPP) (Sokalski & Lewenstam, 2001; Sokalski et al., 2003; Bobacka et al., 2008) or simpler diffusion-layer model (DLM) (Lewenstam et al., 1987; Paczosa-Bator et al., 2007). The time-dependent potential profiles observed experimentally are in excellent agreement with these predicted formally. According to the DLM model, the electrode response depends on the different hydration energy (and mobility) of ions involved in ion-exchange processes. The lower hydration energy of calcium ions (as well as potassium or sodium ions) makes the transport of these ions to and into the membrane faster in comparison to magnesium or lithium, with resulting redistribution of the surface concentration of ions (see Fig. 11). The influx, or outflow, of slower ions determines the speed of the ion-exchange process. This is why, after a change of the e.g. Mg^{2+} ion concentration in the solution bulk, deficiency of e.g. Ca^{2+} ions in the vicinity of the CP-BL-Ca membrane surface vs. bulk is predicted and accordingly a monotonic response type is observed (Fig. 13a). In contrast, after the change of bulk Ca^{2+} ion concentration, the local excess of Mg^{2+} ions at the surface of the CP-BL-Mg membrane is predicted and an overshoot-type response is observed (as shown on Fig. 13b).

Both theoretical models (NPP and DLM) support a fundamental idea of the biomimetic membrane concept presented and show that when a biologically active site is allowed for a competitive ion-exchange the extent of the competition is regulated by the electric potential "applied" to this site and the transport of ions to and from the site. Different E-t patterns have to be observed for faster ions in comparison to slower which is known as "ionic antagonism". Our study shows that a local e.g. magnesium ion concentration increase is

expected when positive vs. equilibrium (rest) potential is applied. In other words it means that magnesium ions leave the coordinating sites and smaller calcium ion is admitted. This is exactly what happens at the neck of magnesium blocked NMDA channel where this ion is attracted by Asn and Gln. When excited by action potential the channel gets unblocked and allows faster calcium ions to pass through (Nowak et al., 1984; Vargas-Caballero & Robinson, 2004). Obviously, deficiency of magnesium in external compartments can facilitate calcium influx and modulation of intracellular calcium concentration. Interestingly, this mechanism and magnesium-calcium antagonism in relation to NMDA receptor channel were recently considered as one possible reason for inflammatory response and metabolic syndrome (Rayssiguier et al., 2006; Mazur et al., 2007). The importance of the effects of Ca^{2+} , Mg^{2+} and ATP and other phosphorylated species on cardiac action potentials was recently as well emphasized (Michailova & McCulloch, 2008). A similar case of a competitive ion mechanism can be in interaction of the exogenous lithium ion with negatively-charged inositol phospholipids which is considered to be relevant in treatment of bipolar disorders (Atack et al., 1995; Gibbons et al., 2008).

Presented here potential-dependent local concentration redistribution of ions at the membrane binding sites undoubtedly adds a new dimension in interpretation of above effects. We address these issues in our present research.

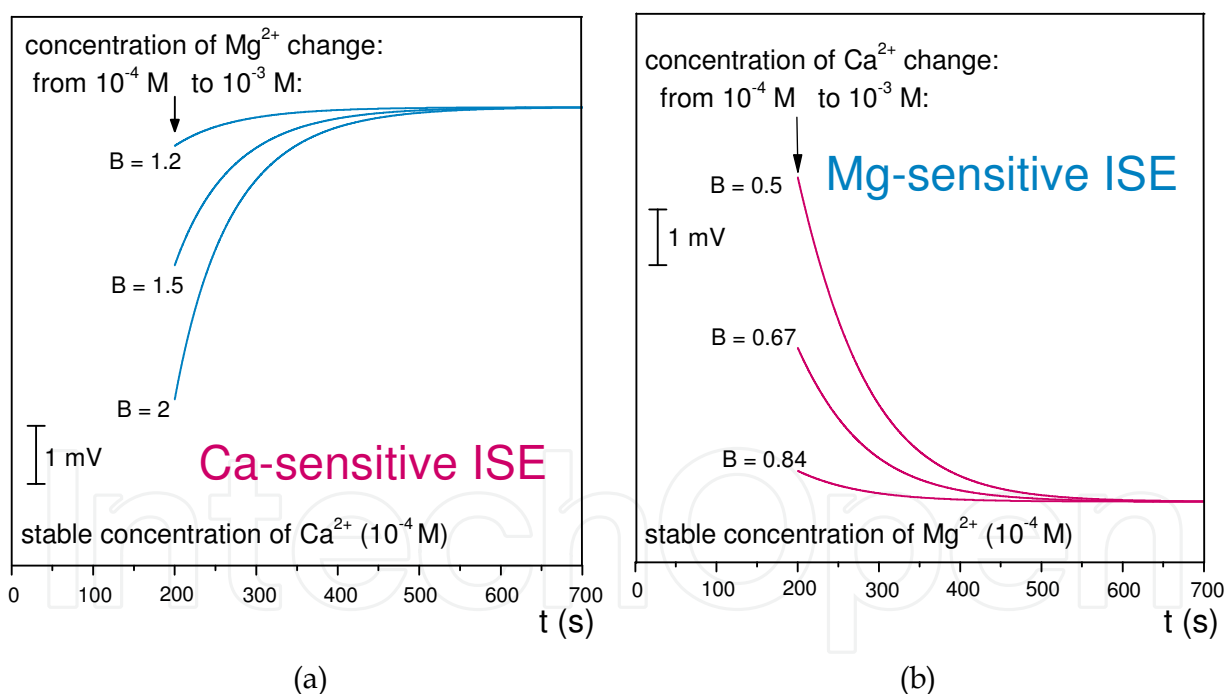


Fig. 13. The time - dependent response of calcium (a) and magnesium (b) sensitive electrode, calculated on the ground DLM model for various B parameter ($B = \bar{U}_{\text{N}^{2+}} / \bar{U}_{\text{Y}^{2+}}$ where $\bar{U}_{\text{N}^{2+}}, \bar{U}_{\text{Y}^{2+}}$ represent the mobilities of ions in the membrane phase and $K_{\text{Y,N}} = 1$): (a) represents response after increase Mg^{2+} activity in the solution of mix magnesium and calcium ions for $B = 1.2, 1.5$ and 2 , (b) potential response after increase Ca^{2+} activity in the solution of mix magnesium and calcium ions for $B = 0.5, 0.67$ and 0.84 .

9. Conclusion

The biomimetic membrane methodology allows visualization and inspection of the competitive and voltage-dependent ion exchange on biologically active sites. By using selected and relevant to real ionic sites of biological membranes and their channels (e.g. ATP, Asn, Gln) it is possible to access the ionic redistribution on the sites in the function of the bulk concentration of ions, external potential and time. In other words, the concept presented provides a tool to study the role of ions and the influence of ion supplementation, ion deficiencies, and ion antagonism on membrane potential. It as well can be a tool for investigating the bias between voltage effects (long-term potentiation (LTP), cardiac arrhythmias, and low-frequency signals in brain) on ionic local (at/on site) or transmembrane redistributions.

10. Acknowledgements

This work is supported by the National Centre for Research and Development (NCBiR). Grant No. DWM/232/MATERA/2006 and KBN Grant R15 005 03.

11. References

- Atack. J.R.; Broughton. H.B. & Pollack. S.J. (1995) Inositol monophosphatase - a putative target for Li⁺ in the treatment of bipolar disorder. *Trends Neurosci*, Vol. 18, No. 8, (343-349), ISSN 0166-2236
- Bobacka. J.; Gao. Z.; Ivaska. A. & Lewenstam A. (1994) Mechanism of ionic and redox sensitivity of p-type conducting polymers. Part 2. Experimental study of polypyrrole. *J Electroanal. Chem.*, Vol. 368, No. 1-2, (33-41), ISSN 0022-0728
- Bobacka. J.; Ivaska. A. & Lewenstam. A. (2008) Potentiometric ion sensors. *Chem. Rev.*, Vol. 108, No. 2, (329-351) ISSN 0009-2665
- Desai. U.R. (2004) New antithrombin-based anticoagulants. *Med. Res. Rev.*, Vol. 24, No. 2, (151-181), ISSN: 0198-6325
- Fraústo da Silva. J.J.R. & Williams. R.J.P. (2001). *The Biological Chemistry of the Elements*, Oxford University Press Inc., ISBN 0198508476, New York USA
- Gao. Z.; Bobacka. J.; Lewenstam. A. & Ivaska. A. (1994) Electrochemical behaviour of polypyrrole film polymerized in indigo carmine solution. *Electrochim. Acta*, Vol. 39, No. 5, 755-762, ISSN 0013-4686
- Gibbons. C.E.; Maldonado-Pérez. D.; Shah. A.N.; Riccardi. D. & Ward. D.T. (2008) Calcium-sensing receptor antagonism or lithium treatment ameliorates aminoglycoside-induced cell death in renal epithelial cells. *Biochim. Biophys. Acta*, Vol. 1782, No. 3, (188-195), ISSN 0005-2736
- Hille. B. (1992) Selective permeability: saturation and binding. In: *Ionic Channels of excitable membranes*, 471-502, Sinauer Associates Inc., ISBN 0878933239, Massachusetts USA
- Lewenstam. A.; Hulanicki. A. & Sokalski. T. (1987) Response mechanism of solid state ion selective electrodes in the presence of interfering ions. *Anal. Chem.*, Vol. 59, No. 11, (1539- 1544), ISSN 0003-2700
- Lewenstam. A.; Bobacka. J. & Ivaska. A. (1994) Mechanism of ionic and redox sensitivity of p-type conducting polymers. Part I. Theory. *J Electroanal. Chem.*, Vol. 368, No. 1-2, (23-31), ISSN 0022-0728

- Maddison, D.S. & Unsworth, J. (1989) Optimization of synthesis conditions of polypyrrole from aqueous solutions. *Synth. Met.*, Vol. 30, No. 1, (47-55), ISSN 0379-6779
- Mazur, A.; Maier, J.A.M.; Rock, E.; Gueux, E.; Nowacki, W. & Rayssiguier, Y. (2007) Magnesium and the inflammatory response: Potential physiopathological implications. *Archiv. Biochem. Biophys.*, Vol. 458, No. 1, (48-56), ISSN 0003-9861
- McBain, C.J. & Mayer, M.L. (1994) N-methyl-D-aspartic acid receptor structure and function. *Physiol. Rev.*, Vol. 74, No. 3, (723-760), ISSN 0031-9333
- Michailova, A. & McCulloch, A.D. (2008) Effects of Mg^{2+} , pH and PCr on cardiac excitation-metabolic coupling. *Magnesium Research*, Vol. 21, No. 1, (16-28), ISSN 0953-1424
- Migdalski, J.; Blaz, T. & Lewenstam, A. (1996) Conducting polymer-based ion-selective electrodes. *Anal. Chem. Acta*, Vol. 322, No. 3, (141-149), ISSN 0003-2670
- Migdalski, J.; Blaz, T., Paczosa, B.; Lewenstam, A. (2003) Magnesium and calcium-dependent membrane potential of poly(pyrrole) films doped with adenosine triphosphate. *Microchim. Acta*. Vol. 143, No. 2-3, (177-185), ISSN 0026-3672
- Niu, L.; Kvarnström, C.; Fröberg, K. & Ivaska, A. (2001) Electrochemically controlled surface morphology and crystallinity in poly(3,4-ethylenedioxythiophene) films. *Synth. Met.*, Vol. 122, No. 2, (425-429), ISSN 0379-6779
- Nowak, L.; Bregestovski, P.; Ascher, P.; Herbet, A. & Prochiantz, A. (1984) Magnesium gates glutamate-activated channels in mouse central neurons. *Nature*, Vol. 307, No. 5950, (462-465), ISSN 0028-0836
- Paczosa, B., Blaz, T., Migdalski, J. & Lewenstam, A. (2004) Conducting polymer films as model biological membranes. Electrochemical and ion-exchange properties of PPy and PEDOT films doped with heparin. *Polish J Chem.* Vol. 78. No. 9. (1543-1552). ISSN 0137-5083.
- Paczosa-Bator, B.; Migdalski, J. & Lewenstam, A. (2006) (a) Conducting polymer films as model biological membranes. Electrochemical and ion-exchange properties of poly(pyrrole) films doped with asparagine and glutamine. *Electrochim. Acta*, Vol. 51, No. 11, (2173-2181), ISSN 0013-4686
- Paczosa-Bator, B.; Peltonen, J.; Bobacka, J. & Lewenstam, A. (2006) (b). Influence of morphology and topography on potentiometric response of magnesium and calcium sensitive PEDOT films doped with adenosinetriphosphate (ATP). *Anal. Chim. Acta*, Vol. 555, No. 1, (118-127), ISSN 0003-2670
- Paczosa-Bator, B., Blaz, T., Migdalski, J. & Lewenstam, A. (2007) Conducting polymers in modelling transient potential of biological membranes. *Bioelectrochemistry*, Vol. 71, No. 1, (66-74), ISSN 1567-5394
- Paczosa-Bator, B.; Stepień, M., Maj-Zurawska, M & Lewenstam, A. (2009). Biomimetic study of the Ca^{2+} - Mg^{2+} and K^{+} - Li^{+} antagonism on biologically active sites - new methodology to study potential dependent ion exchange. *Magnesium Research*, Vol. 22, No. 1, (10-20), ISSN 0953-1424
- Rayssiguier, Y.; Gueux, E.; Nowacki, W.; Rock, E. & Mazur, A. (2006) High fructose consumption combined with low dietary magnesium intake may increase the incidence of the metabolic syndrome by inducing inflammation. *Magnesium Research*, Vol. 19, No. 4, (237-243), ISSN 0953-1424
- Saris, N.E.; Mervaala, E.; Karppanen, H.; Khawaja, J.A. & Lewenstam, A. (2000). *Clin. Chim. Acta*, Vol. 294, No. 1-2, (1-26), ISSN 0009-8981

- Sokalski. T. & Lewenstam. A. (2001) Application of Nernst-Planck and Poisson equations for interpretation of liquid-junction and membrane potentials in real-time and space domains. *Electrochem. Comm.*, Vol. 3, No. 3, (107-112), ISSN 1388-2481
- Sokalski. T.; Lingenfelter. P. & Lewenstam. A. (2003) Numerical solution of the coupled Nernst-Planck and Poisson equations for liquid-junction and ion-selective membrane potentials. *J Phys. Chem. B*, Vol. 107, No. 11, (2443-2452), ISSN 1089-5647
- Unsworth. J.; Innis. P.C.; Lunn. B.A. & Norton G.P. (1992) The influence of electrolyte pH on the surface morphology of polypyrrole. *Synth. Met.*, Vol. 53, No. 3, (59-69) ISSN 0379-6779
- Vargas-Caballero. M. & Robinson. H.P.C. (2004) Fast and slow voltage-dependent dynamics of magnesium block in the NMDA receptor: The asymmetric trapping block model. *J Neuroscience*, Vol. 24, No. 27, (6171-6180), ISSN 0270-6474

IntechOpen



Advances in Biomimetics

Edited by Prof. Marko Cavrak

ISBN 978-953-307-191-6

Hard cover, 522 pages

Publisher InTech

Published online 26, April, 2011

Published in print edition April, 2011

The interaction between cells, tissues and biomaterial surfaces are the highlights of the book "Advances in Biomimetics". In this regard the effect of nanostructures and nanotopographies and their effect on the development of a new generation of biomaterials including advanced multifunctional scaffolds for tissue engineering are discussed. The 2 volumes contain articles that cover a wide spectrum of subject matter such as different aspects of the development of scaffolds and coatings with enhanced performance and bioactivity, including investigations of material surface-cell interactions.

How to reference

In order to correctly reference this scholarly work, feel free to copy and paste the following:

Beata Paczosa-Bator, Jan Migdalski and Andrzej Lewenstam (2011). Biomimetic Membranes as a Tool to Study Competitive Ion-Exchange Processes on Biologically Active Sites, *Advances in Biomimetics*, Prof. Marko Cavrak (Ed.), ISBN: 978-953-307-191-6, InTech, Available from: <http://www.intechopen.com/books/advances-in-biomimetics/biomimetic-membranes-as-a-tool-to-study-competitive-ion-exchange-processes-on-biologically-active-si>

INTECH
open science | open minds

InTech Europe

University Campus STeP Ri
Slavka Krautzeka 83/A
51000 Rijeka, Croatia
Phone: +385 (51) 770 447
Fax: +385 (51) 686 166
www.intechopen.com

InTech China

Unit 405, Office Block, Hotel Equatorial Shanghai
No.65, Yan An Road (West), Shanghai, 200040, China
中国上海市延安西路65号上海国际贵都大饭店办公楼405单元
Phone: +86-21-62489820
Fax: +86-21-62489821

© 2011 The Author(s). Licensee IntechOpen. This chapter is distributed under the terms of the [Creative Commons Attribution-NonCommercial-ShareAlike-3.0 License](#), which permits use, distribution and reproduction for non-commercial purposes, provided the original is properly cited and derivative works building on this content are distributed under the same license.

IntechOpen

IntechOpen